A Family of Electroluminescent Silyl-Substituted Poly(*p*-phenylenevinylene)s: Synthesis, Characterization, and Structure−Property Relationships

Z.-K. Chen and W. Huang*

Institute of Materials Research and Engineering (IMRE), National University of Singapore, 3 Research Link, Singapore 117602, Republic of Singapore

L.-H. Wang and E.-T. Kang

Department of Chemical and Environmental Engineering, National University of Singapore, 10 Kent Ridge Crescent, Singapore 119260, Republic of Singapore

B. J. Chen, C. S. Lee, and S. T. Lee

Department of Physics and Materials Science, City University of Hong Kong, Tat Chee Avenue, Kowloon, Hong Kong, People's Republic of China

Received March 30, 2000; Revised Manuscript Received August 18, 2000

ABSTRACT: A series of intense photoluminescent (PL) polymers containing silyl groups with chain length from C1 to C18 has been successfully synthesized through polycondensation reaction. Introducing silyl groups into a conjugated polymer affords the polymer good processability, amorphousness, good film-forming ability, and sharp emission. A systematic analysis of this series of polymers indicates that increasing the side chain length of the polymers will slightly lower the thermal stability while increasing the molecular weight. UV−vis absorption and PL emission spectra of the polymers are quite similar. Cyclic voltammetric (CV) investigation of the polymers reveals that the side chain length plays an important role in the redox behavior of the polymers. Shorter side chain polymers possess better reproducibility of CV scans and higher peak currents, which implies that the chemical/electrical stability and charge injection and/or transporting ability for shorter side chain polymers are better than those for longer ones. Devices fabricated from poly[2,5-bis(decyldimethylsilyl)-1,4-phenylenevinylene] (DS-PPV) with the configuration of ITO/DS-PPV/Mg:Ag and ITO/PEDOT:PSS/DS-PPV/Mg:Ag indicate that the hole injection is the determining factor for device performance. Addition of the hole injection layer can improve the current efficiency and power efficiency by about 7 times and lower the turn-on voltage from 7.5 to 4.0 V for the two types of devices.

Introduction

Electroluminescent (EL) polymers have been extensively studied in the past few years owing to their promising applications in polymeric light-emitting diodes (PLEDs), photovoltaic diodes, lasers, and field emission transistors (FETs).[1−3] In particular, application in PLEDs has attracted significant attention following the first report of the PLED device based on poly(*p*-phenylenevinylene) (PPV) in 1990,[4] mainly because of their fascinating perspectives of low-cost processing through simple spin-coating or casting technique, various emission colors sweeping the full range of the visible spectrum, low driving voltages and ease of realizing large area displays, and flexible structures. The accomplishments of PLEDs require efforts in the design and synthesis of electroluminescent polymers with tailored properties such as high photoluminescent (PL) quantum efficiency, good processability, and high thermal/optical/electrical stability. So far, numerous conjugated polymers have been successfully synthesized as the active layers and/or transporting layers for PLEDs such as PPV and its derivatives, poly(*p*-phenylene)s (PPP), polythiophenes (PTs), and polyfluorenes (PFs) as well as their copolymers.[5−11] Among them, PPV and their alkyl or alkoxy derivatives are the most commonly used materials for PLEDs on account of their good device performance.

Recently, there has been increasing interest in the silyl-substituted luminescent polymers, in which silyl moieties are introduced either as side chains or as a segment integrated into the polymer backbones.[12−14] Incorporating silylene or oligosilylene segments into a polymer backbone has the advantage of confinement of the electron delocalization over the polymer chain by alternating delocalized σ-bonds and π-bonds to realize high quantum efficiency emission while improving the flexibility of the resulting copolymers.[15,16]

Unlike organosilicon copolymers, silyl groups as side chains attached to a conjugated polymer backbone such as PPV are seldom reported. A systematic study on the synthesis of polymers combining silyl side chains and PPV skeleton and the effect of substitution on the chemical, physical, and optoelectronic properties of the polymers is interesting to materials scientists and synthetic organic chemists. In 1994, Wudl and co-workers reported the first silylated PPV—poly(2-cholestanoxy-5-thexyldimethylsilyl-1,4-phenylenevinylene) (CS-PPV), which is a green-light-emitting material.[17] Based on the silylated polymer, improved quantum efficiency of LED devices was observed.[18] The attractive properties of silyl-substituted PPVs are their extremely high PL quantum efficiency, good solubility, and uniform film morphology in the film state.[19,20] Indeed, very high PL efficiency of

* Corresponding author. Telephone: (65) 874 8592. FAX: (65) 872 0785. E-mail: wei-huang@imre.org.sg.

10.1021/ma0005670 CCC: $19.00
Published on Web 11/02/2000

film samples (60% or above) and EL efficiency of a PPV derivative with one silyl substituent were demonstrated by Holmes and Friend et al.[20] Their subsequent work concerning Si-containing PPV copolymers prepared from silyl-bearing monomers and alkoxy-substituted monomers indicated that the PL and EL efficiencies of resulting copolymers were determined by the feed ratio of the two comonomers. The higher the ratio of the silicon-containing monomer involved, the higher efficiencies the polymers exhibited.[21] This result suggests that introducing more silyl groups than alkoxy pendants into the polymer as side chains can improve the polymer quantum efficiencies.

It is reported that incorporation of more silylene component into the polymer backbone can affect the polymer supramolecular structure. The film structure will be changed from ordered or semiordered to disordered state as the Si component increases.[13a] It can be expected that the bis-silyl substitution will afford the PPV further improved amorphousness, which is crucial for the development of luminescent materials for PLED applications. Therefore, it is meaningful to design and synthesize bis-silyl substituted PPVs with the aim of keeping or even further enhancing the PL efficiency and simultaneously improving the processability by a highly branched side chain structure and flexiblility of silyl groups associated with the larger atom size of Si and the longer bond length of C−Si.[22]

In this contribution we report the synthesis of a family of bis-silyl-substituted PPVs with different side chain lengths ranging from C1 to C18. The effects of the specific Si substitution and the side chain length on molecular weight, molecular morphology, thermal stability, absorption and emission spectra, and electrochemical behavior have been investigated and will be discussed. In addition, the energy levels of the highest occupied molecular orbitals (HOMO) and lowest unoccupied molecular orbitals (LUMO) of the polymers have been measured by means of cyclic voltammetry (CV). Such information is useful for the design of the LED device structure with efficient injection and transport of charge carriers.

Experimental Section

Measurements. NMR spectra were collected on a Bruker ACF-300 or Bruker AMX-500 spectrometers with chloroform-*d* as solvent and tetramethylsilane as internal standard. FT-IR spectra were recorded on a Bio-Rad FTS 165 spectrometer by dispersing samples in KBr disks. UV−vis and fluorescence spectra were obtained on a Shimadzu UV−VIS−NIR 3101 spectrophotometer and on a Perkin-Elmer LS 50B luminescence spectrometer, respectively. Thermogravimetric analysis (TGA) was conducted on a DuPont Thermal Analyst 2100 system with a TGA 2950 thermogravimetric analyzer under a heating rate of 20 °C/min and an air flow rate of 75 mL/min. Differential scanning calorimetry (DSC) was run on a DuPont DSC 2910 module in conjunction with the DuPont Thermal Analyst system. Elemental microanalyses were performed on a Perkin-Elmer 2400 elemental analyzer for C, H, N, and Br determination. Cyclic voltammetry was performed on an EG&G Parc Model 273A potentiostat/galvanostat system with a three-electrode cell in a solution of Bu_4NBF_4 (0.10 M) in acetonitrile at a scan rate of 10 mV/s. Polymer films were coated on a square Pt electrode (0.50 cm^2) by dipping the electrode into the corresponding solutions and then drying in argon. A Pt wire was used as the counter electrode and a Ag/$AgNO_3$ (0.10 M in acetonitrile) electrode was used as the reference electrode. Prior to each series of measurements, the cell was deoxygenated with argon. Gel permeation chromatography (GPC) analysis was conducted on a Perkin-Elmer model 200 HPLC system equipped with Phenogel MXL and MXM columns, using polystyrene as standard and THF as eluent. X-ray diffraction measurements of film samples prepared through spin coating the chloroform solutions of the polymers were performed on Philips X'pert-MPD spectrometer.

Single-layer and double-layer LED devices were fabricated on glass substrates coated with indium−tin oxide (ITO) with a sheet resistance of 150 Ω/□. The substrate was cleaned by sonicating in hexane and 2-propanol successively prior to use. The hole injection layer of poly(3,4-ethylenedioxythiophene) (PEDOT) doped with poly(styrenesulfonic acid) (PSS) (PEDOT:PSS) was prepared from a water dispersion and baked at 105 °C for 20 min with the thickness of 30 nm. The light-emitting layer (60 nm thick) of DS-PPV was spin coated from a chloroform solution on ITO surface or on the hole injection layer. Finally, a 200-nm-thick Mg:Ag (10:1 by mass) cathode was vacuum deposited onto the DS-PPV film at a pressure below 5×10^{-4} Pa. The emitting areas of the EL devices are 2×3 mm^2. EL spectra of the devices were measured with a PR650 SpectraScan photospectrometer. Luminance−current density−voltage (L−I−V) characteristics were recorded simultaneously with the measurement of the EL spectra by attaching the photospectrometer to a Keithley 236 programmable voltage−current source. All measurements were carried out at room temperature under ambient atmosphere.

Materials. Tetrahydrofuran (THF) was distilled over sodium/benzophenone. 2,5-Dibromo-*p*-xylene, potassium *tert*-butoxide (1.0 M solution in THF), *N*-bromosuccinimide (NBS), and magnesium turnings were purchased from Aldrich. Trimethylsilyl chloride, butyldimethylsilyl chloride, decyldimethylsilyl chloride, dimethyldodecylsilyl chloride, and dimethyloctadecylsilyl chloride were obtained from Fluka. All chemicals were used without further purification.

Synthesis of 2,5-Dibromo-*p*-xylene (1).[23] A 21.2 g sample (0.20 mol) of *p*-xylene, 0.39 g (2.4 mmol) of ferric chloride, and 0.13 mL of deionized water were charged into a 100 mL three-neck flask, equipped with a thermometer and a condenser with gas outlet. A 41.6 g sample (0.26 mol) of bromine was added dropwise to the mixture with stirring at 0−5 °C. The mixture was kept at this temperature for 2 h and then was warmed to ambient temperature with stirring. When hydrogen bromide evolution ceased, the reaction was quenched and the mixture was washed with water; then monobromo-*p*-xylene was distilled off under vacuum pressure. The crude product was recrystallized from hexane to afford 14.4 g of white crystals (yield 91%). Mp 72.0−73.5 °C (lit. 72−74 °C). ^{1}H NMR (300 MHz, $CDCl_3$, ppm): δ 2.33 (6H, s), 7.39 (2H, s).

Synthesis of 2,5-Bis(decyldimethylsilyl)-*p*-xylene (2c).[24] The Grignard reagent of 2,5-bis(bromomagnesio)-*p*-xylene was prepared by refluxing the mixture of **1** (5.28 g, 20.0 mmol) and magnesium turnings (1.06 g, 44.0 mmol) in 40 mL of anhydrous THF for 4 h. To this solution, cooled in an ice bath, was added a solution of decyldimethylsilyl chloride (12.2 mL, 45.0 mmol) in 40 mL of THF. The mixture was refluxed for 24 h and then cooled in an ice bath. After quenching with saturated ammonium chloride aqueous solution, THF was evaporated and the residue was extracted with 30 mL of hexane three times. The combined organic layer was washed with water and brine and then dried over anhydrous magnesium sulfate. After the solvent was evaporated under reduced pressure, the residue was purified through silicon-gel chromatography eluted with hexane to afford 5.69 g of a colorless liquid with a yield of 57%. Meanwhile, 1.65 g of byproduct of 2-decyldimethylsilyl-*p*-xylene was also obtained. MS: 502. ^{1}H NMR (300 MHz, $CDCl_3$, ppm): δ 0.29 (12H, s, $-Si(CH_3)_2$), 0.79 (4H, t, $-SiCH_2-$), 0.88 (6H, t, $-CH_3$), 1.25−1.32 (32H, m, $-(CH_2)_8-$), 2.39 (6H, s), 7.19 (2H, s). Anal. Calcd for $C_{32}H_{62}Si_2$: C, 76.41; H, 12.42. Found: C, 76.56; H, 12.23.

2a, **2b**, **2d**, and **2e** were synthesized, purified and characterized in a similar manner. Details can be found in the Supporting Information.

Synthesis of 2,5-Bis(decyldimethylsilyl)-1,4-bis(bromomethyl)benzene (3c). A 1.00 g sample (2.0 mmol) of **2c**, 0.78 g (4.4 mmol) of *N*-bromosuccinimide (NBS), catalytic

amounts of benzoyl peroxide (BPO), and 60 mL of benzene were charged in a 100 mL flask. The mixture was stirred at ambient temperature under tungsten light for 2 h. The solution was then washed with water three times and with brine. The organic phase was dried over anhydrous magnesium sulfate. After filtration, the solvent was evaporated, and the residue was purified through silicon-gel chromatography eluted by hexane to afford 0.61 g of a colorless liquid (yield 46%). The product will solidify as wax on standing. Mp 35.0−36.0 °C. MS: 660. FT-IR (KBr) ν_{max}/cm^{-1}: 3077, 3004, 2956, 2917, 2855, 1468, 1411, 1344, 1251, 1207, 1190, 1170, 1125, 1004, 883, 864, 836, 819, 790, 759, 720, 702, 681, 660, 650, 538, 477, 457, 438. ^{1}H NMR (300 MHz, $CDCl_3$, ppm): δ 0.38 (12H, s, $-Si(CH_3)_2$), 0.85−0.87 (10H, m, $-SiCH_2-$, $-CH_3$), 1.24−1.31 (32H, m, $-(CH_2)_8-$), 4.58 (4H, s, $-CH_2Br$), 7.49 (2H, s). ^{13}C NMR (75.5 MHz, $CDCl_3$, ppm): δ 142.0, 140.0, 137.5, 34.1, 33.4, 31.8, 29.6, 29.5, 29.3, 29.2, 23.8, 22.6, 16.3, 14.0, −1.6. Anal. Calcd for $C_{32}H_{60}Br_2Si_2$: C, 58.16; H, 9.15; Br, 24.18. Found: C, 57.98; H, 9.01; Br, 23.86.

The synthesis, purification, and characterization of **3a**, **3b**, **3d**, and **3e** are similar with that of **3c**, and details can be found in the Supporting Information.

Synthesis of Poly[2,5-bis(decyldimethylsilyl)-1,4-phenylenevinylene] (4c) (DS-PPV).[25] A solution of 0.500 g (0.76 mmol) of **3c** in 25 mL of anhydrous THF was charged in a 50 mL flask. To this stirred solution was added dropwise 5 mL of 1.0 M solution of potassium *tert*-butoxide (5.0 mmol) in anhydrous THF at room temperature. The mixture was continuously stirred for 24 h. The reaction mixture was then poured into 200 mL of methanol with stirring. The resulting yellow precipitate was collected and dissolved in chloroform and reprecipitated in methanol twice more. The polymer was followed by extracting through a Soxhlet extractor with methanol and acetone for 12 h successively and dried under vacuum to afford 0.239 g (63% yield) of a yellow polymer. FT-IR (KBr) ν_{max}/cm^{-1}: 3057, 2956, 2923, 2852, 1465, 1249, 1162, 1108, 960, 835, 768, 721, 641, 526, 464. ^{1}H NMR (500 MHz, $CDCl_3$, ppm): δ 0.20−0.55 (12H, s, $-Si(CH_3)_2$), 0.74−0.88 (6H, t, $-CH_3$), 0.88−1.02 (4H, br, $-SiCH_2-$), 1.02−1.46 (32H, m, $-(CH_2)_8-$), 7.32−7.68 (2H, br), 7.68−8.08 (2H, br, $-CH=CH-$). ^{13}C NMR (126 MHz, $CDCl_3$, ppm): δ 151.4, 135.7, 128.2, 125.4, 33.6, 31.8, 30.2, 29.6, 29.3, 24.1, 22.6, 21.1, 16.7, 14.0, −1.4. Anal. Calcd for $(C_{32}H_{58}Si_2)_n$: C, 77.03; H, 11.72. Found: C, 76.82; H, 11.39.

4a, **4b**, **4d**, and **4e** were synthesized, purified and characterized in a similar manner. Details can be found in the Supporting Information.

Results and Discussion

The synthetic procedure for the silyl-substituted PPVs (Si-PPVs) is depicted in Scheme 1. All four steps are facile and can be easily controlled. During the synthesis of disilyl-*p*-xylene, 2,5-dibromo-*p*-xylene can be converted to the Grignard reagent in THF with a quite high yield (> 90%). However, the coupling of the Grignard reagent to the silyl chloride is not very efficient, which may be associated with the bulky structure of the dimethylalkylsilyl group. Therefore, excess silanizing reagent is required to improve the yield of the disubstituted product. Normally there is about 20%−30% of the Grignard reagent coupled with only one silyl chloride to afford the monosubstituted byproduct. The monomers were prepared through the radical bromination of compound **2**, which were promoted by radical initiator (BPO). The optimum ratio of NBS is 2.2 equiv to the disilyl-*p*-xylene used, which can afford the product with yields of 40%−50%. Excess NBS will lead to multibromination and even replace the silyl group on the phenylene ring. For example, when 1 mol of 2,5-bis(trimethylsilyl)-*p*-xylene (**2a**) reacted with 2.8 mol of NBS for 3.5 h, the dominant product was 2-bromo-5-trimethylsilyl-1,4-bisbromomethylbenzene (yield 36%).

Scheme 1. Synthetic Route for Silyl Derived PPVs[a]

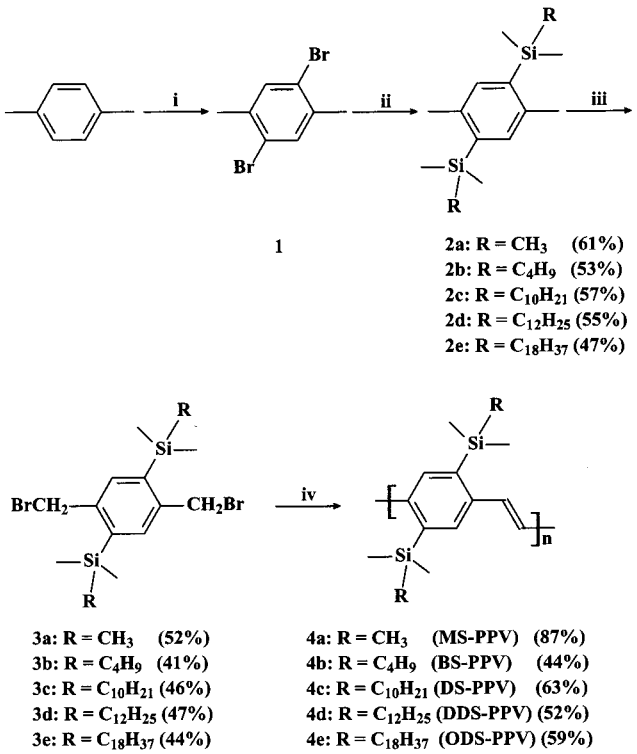

[a] Reagents and conditions: (i) $Br_2/FeCl_3 \cdot 3H_2O$; (ii) Mg/THF/$R(CH_3)_2SiCl$; (iii) NBS/benzene/BPO/hν; (iv) KOBu^t/THF.

The formation of the byproduct is due to the electrophilic substitution of the trimethylsilyl group by bromine on NBS, which is competitive with the radical reaction.[26] The monomers can be easily polymerized through the Gilch route using potassium *tert*-butoxide as base in dry THF in ambient conditions.

The obtained polymers are yellow to orange-yellow solids after precipitation of their chloroform solutions in methanol twice. The collected polymers were further purified by Soxhlet extraction through methanol and acetone to remove the small molecules, water and inorganic impurities. All the polymers, except MS-PPV, are fully soluble in conventional organic solvents such as chloroform, THF, toluene, 1,1,2,2-tetrachloroethane, and xylene. MS-PPV only shows very weak solubility in xylene. The excellent solubility of the polymers, compared to alkyl- or alkoxy-substituted PPVs, is attributed to the silyl pendant, which has two methyl groups and one long alkyl chain and facilitates the polymer good processability. Solution processability for fabricating LED devices is one of the most attractive advantages of polymers over small organic molecule based LEDs or inorganic LEDs. Unfortunately, the solubility of most luminescent polymers investigated so far is not as good as required. For example, poly[2-methoxy-5-(2′-ethylhexyloxy)-1,4-phenylenevinylene] (MEH-PPV), a well-investigated PPV derivative, is said to possess a satisfactory solubility in common organic solvents. However, part gel or microgel has always been found during the polymerization process. Especially when the polymer is prepared from the bisbromomethyl monomer through the Gilch route, the gel phenomenon is even more critical. Currently, there is a trend to introduce highly branched side chains into polymers to improve the processability. Poly[2-methoxy-5(3′,7′-dimethyloctyloxy)-1,4-phenylenevinylene] (OC_1C_{10}-PPV) and poly[2,5-bis(3′,7′-dimethyloctyloxy)-1,4-phenylenevi-

Table 1. Physical and Thermal Properties of Si-PPVs

						wt loss of the first step		
polymer	M_n/M_w	polydispersity	T_d (onset, °C)	T_d[5] (°C)	wt loss at 400 °C (%)	temp range (°C)	lost segment	expertl/calcd (%)
MS-PPV			310	335	22.6	310−411	$-Si(CH_3)_3$	30/29.5[a]
BS-PPV	73 400/187 400	2.55	312	392	5.3	312−526	$-Si(CH_3)_2C_4H_9$, $-C_4H_9$	56/52
DS-PPV	117 700/239 100	2.03	310	371	7.2	310−553	$-Si(CH_3)_2C_{10}H_{21}$, $-C_{10}H_{21}$	68/68
DDS-PPV	152 600/352 000	2.31	294	377	9.0	294−521	$-Si(CH_3)_2C_{12}H_{25}$, $-C_{12}H_{25}$	77/72
ODS-PPV	227 700/416 900	1.83	294	362	12.3	294−508	$-Si(CH_3)_2C_{18}H_{37}$, $-C_{18}H_{37}$	78/78

[a] For MS-PPV, the experimental and calculated weight losses at the end of the second step corresponding to the decomposition of both the trimethylsilyl groups are 58% and 59%, respectively.

nylene] have been reported recently, which showed electrical behavior identical to that of MEH-PPV but improved processability and film-forming ability.[27] The silyl-substituted PPVs also have the similar property as that of OC_1C_{10}-PPV with the branched structure of the side chains, and actually better than the latter because the branched groups close to the polymer backbone lead to effective separation between the polymer chains. Moreover, compared with alkyl- or alkoxy-substituted PPVs, the side chains linked to the polymer backbone through the silicon atom can enhance the flexibility of the polymer, due to the larger atom size of silicon than carbon or oxygen and the longer bond length of Si−C than C−C or C−O. Si atom is about 50% larger than carbon, and the bond length of Si−C is 1.90 Å, while C−C bond length is 1.54 Å.[22] The larger atom size and longer bond length result in lower barriers to Si−C bond rotation, which leads to enhanced flexibility of the polymer. Therefore, we can draw the conclusion that the highly branched side chain structure as well as the replacement of side chains by silyl groups contributes to the satisfactory solubility of the resulting polymers. Si− PPVs have also shown good film-forming ability on both ITO substrates and metal plates. X-ray diffraction investigation of the thin film samples spin-coating from the chloroform solutions at room temperature shows only a very broad band from 5 to 40° for all the polymers, revealing that the polymers are amorphous. Thus, it can be induced that introduction of trialkylsilyl groups into PPV or other conjugated luminescent polymers can improve the solubility and film quality of the polymers.

Molecular weights of the polymers were measured by means of GPC using THF as eluent and polystyrene as standard. The number-average molecular weight (M_n), weight-average molecular weight (M_w), and polydispersity index (PDI) are summarized in Table 1. It can be seen that with increase of the side chain length from C4 for BS-PPV to C18 for ODS-PPV, M_n and M_w are increased from 73 400 and 187 400 to 227 700 and 416 900, respectively, with the polydispersity index ranging from 2.55 to 1.83.

The chemical structure of the polymers was confirmed by FT-IR and NMR spectroscopy. Figure 1 shows the typical FT-IR spectra of DS-PPV and the corresponding monomer **3c**. The vibration bands at 3000−3070 cm^{-1} can be assigned to the ν_{C-H} on the aromatic ring or the vinylene group. The absorption peaks at 2850−2960 cm^{-1}, due to the asymmetric and symmetric stretching of methyl and methylene groups, were observed for both the monomer and polymer. The strong absorption band at about 1470 cm^{-1} is due to the phenylene ring stretch, which is overlapped by the CH_2 scissoring mode. The characteristic absorption band for $Si-CH_3$ was observed at 1241 cm^{-1} with a very sharp peak and strong

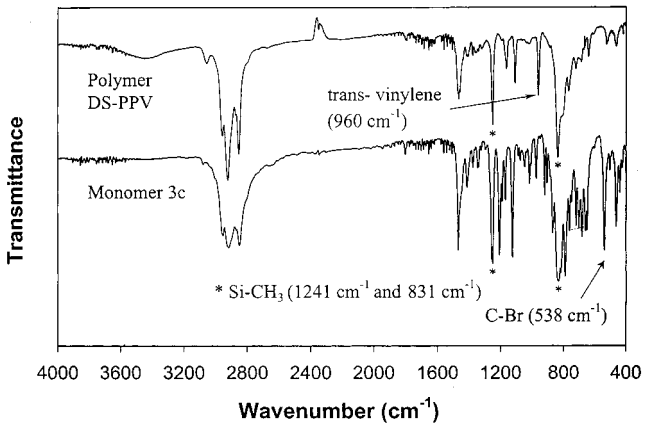

Figure 1. FT-IR spectra of polymer DS-PPV and its monomer.

intensity for all the polymers and the monomers. Another intense band at 831 cm^{-1} is due to the methyl rocking and Si−C stretching vibrations.[28] The specific stretching absorption band for C−Br in the monomer at 538 cm^{-1} totally disappeared after polymerization, while a new band with strong intensity occurred at 960 cm^{-1}, which is due to the C−H out-of-plane deformation of the trans-disubstituted vinylene group. This result suggests that the vinylene group formed through Gilch route is in the trans configuration.

The ^1H NMR and ^{13}C NMR spectra of the polymers were measured except for MS-PPV due to its poor solubility in organic solvent. The spectra of DS-PPV, as an example, are depicted in Figure 2. In Figure 2A, it can be seen that there are two broad peaks at around 7.90 and 7.45 ppm, which are assigned to the protons on the *trans*-vinylene segments and the phenylene rings, respectively. Compared with carbon analogues, the chemical shifts for the methyl and methylene groups linked to silicon on the side chains appeared at a rather high field region (0.46 and 0.95 ppm, respectively), owing to the shielding effect of silicon to the linked $-CH_3$ and $-CH_2$.[29] It is noted that a very weak peak around 3.0 ppm is observed. This signal originates from the resonance of bisbenzyl moieties, which is a type of structural defect in the poly(*p*-phenylenevinylene) backbone. Such defects are formed by the head-to-head linkage of the *p*-xylylene intermediates during polymerization. It is reported that the bisbenzyl as well as diphenylacetylene moieties are the main structural defects of substituted PPVs prepared through the Gilch route.[30] In this work, the amount of bisbenzyl defects is calculated to be around 1.5% for DS-PPV and its analogues based on the integration of the NMR peak area, which is comparable to standard dialkoxy PPV such as MEH-PPV and OC_1C_{10}-PPV, but much better than some asymmetrical phenyl-substituted PPVs.[31] It is believed that the content of structural defects in polymer chains intensely

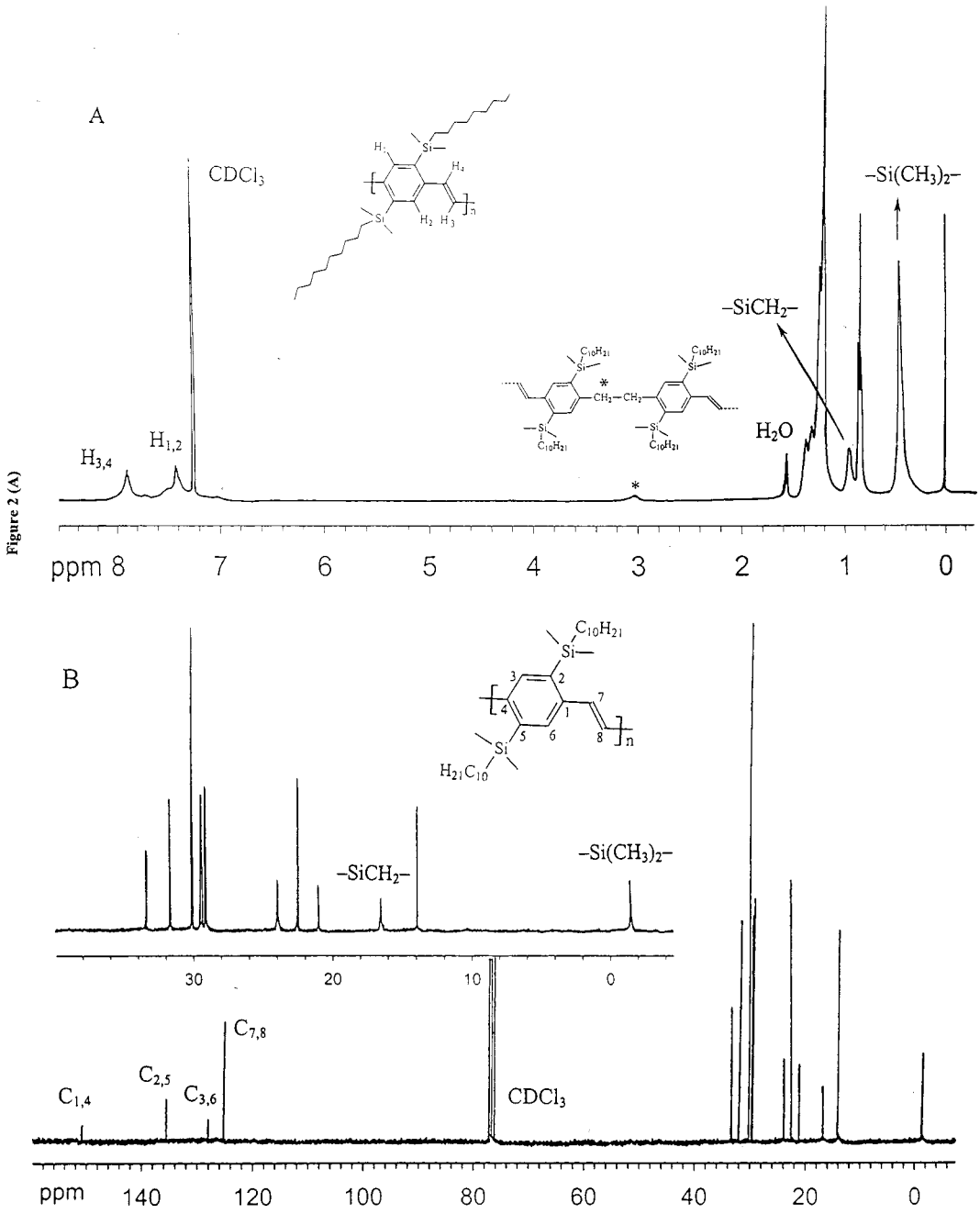

Figure 2 (A)

Figure 2. 500 MHz ^{1}H NMR (A) and ^{13}C NMR (B) spectra of DS-PPV.

affects the device lifetime. Bis-silylated PPV only presents a low level of bisbenzyl moieties in the polymer backbone. Figure 2B shows the ^{13}C NMR of DS-PPV. The resonances of alkyl carbon atoms adjacent to silicon are recognized as easily as its attached protons, which also appeared at a high field region due to the unusual shielding effect of silicon to the carbons. The effect of the silyl groups on the phenyl ring is different from those of analogous carbon-containing functional groups. It demonstrates a strong deshielding effect on both the linked site and the ortho position on the phenyl ring, thus leading to the resonance of C_1 and C_4 appearing at the lowest field. Meanwhile, the chemical shifts for $C_{2,5}$ and $C_{3,6}$ are also higher than those of alkoxy-substituted PPVs. The assignment of the aromatic carbons was based on the comparison of the experimental results with the calculation data of the chemical shifts.[29,32] In the ^{13}C NMR spectra for DS-PPV as well as the others in the series, no signal related to bisbenzyl moieties was observed, which should be due to the quite low content of the segment in the polymer and weak resonance. No information for diphenylacetylene is observed in NMR and FT-IR measurements. Other defects such as carbonyl group, which is recognized as the exciton trapping site in the active layer of PLEDs, are not found in the silyl-derived PPVs.

The thermal stability of the polymers in air was evaluated through TGA. All the polymers reveal the onset degradation temperature at around 300 °C, as shown in Table 1 and Figure 3. When the side chain length increased from C10 to C12 or C18, the onset degradation temperature decreased to 294 °C. It is obvious that the stability will be lowered when introducing longer side chains into the PPVs, which can be induced from the onset degradation temperature, the 5% weight loss temperature, and the weight loss per-

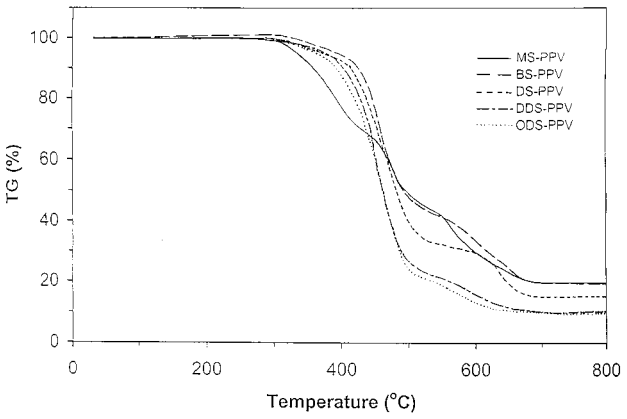

Figure 3. Thermogravimetric analysis (TGA) of Si-PPVs in air.

centage at 400 °C. However, MS-PPV is not in line with the trend and shows rapid decomposition speed in the first stage, which may be related to its lower molecular weight. The weight-loss patterns are also quite similar for polymers with long side chains, which demonstrate a two-step decomposition process, whereas MS-PPV shows its specific character with a three-step pattern, which corresponds to the loss of the first trimethylsilyl group, the loss of second silyl group, and the backbone degradation, respectively. It seems that the long side chain bearing polymers undergo a different pathway for thermolysis. From the percentage of weight loss consideration, it suggests that the polymers lose one of the silyl side groups in the first stage; meanwhile the long aliphatic chain linked to the other silyl group was also decomposed. From Table 1, it can be seen that the experimental results are in good agreement with the calculated weight-loss percentage based on the proposed decomposition routes. The coupling analysis of TGA and FT-IR measurement confirms the above hypothesis. The thermal degradation residues of the Si-PPVs under heating in air from 30 °C to the temperature of the end of the first stage of weight loss were collected and followed by FT-IR investigation. The IR spectra indicate that the long aliphatic chains linked to the silicon atom were completely decomposed. However, the observation of weak absorption bands at 2963 and 2922 $^{-1}$ as well as the band at 1268 cm^{-1} suggests that $Si-CH_3$ still exists in the residue. In addition, carbonyl groups associated with the absorption band at 1698 cm^{-1} appeared in medium intensity owing to the oxidation of carbon in air.

DSC analyses revealed that no phase transition for Si-PPVs was observed from − 50 to 280 °C, which indicates that the polymers possess completely amorphous structures. This result is in agreement with the observation of X-ray diffraction of the spin-coated polymer films.

UV−vis absorption and photoluminescence (PL) spectra of the polymers in dilute solutions of chloroform and as thin films are measured and showed in Figure 4. The maximum UV−vis absorption takes place at about 435 nm for all the solution samples. The film sample of BS-PPV shows the same λ_{max} as the solution one, which implies that the conformations in the two states are quite similar although the absorption band is a little broader in the solid state. Polymers with longer side chains in the film states are bathochromically shifted compared to their solution samples. The longer the side chain, the broader the absorption peak appears. The

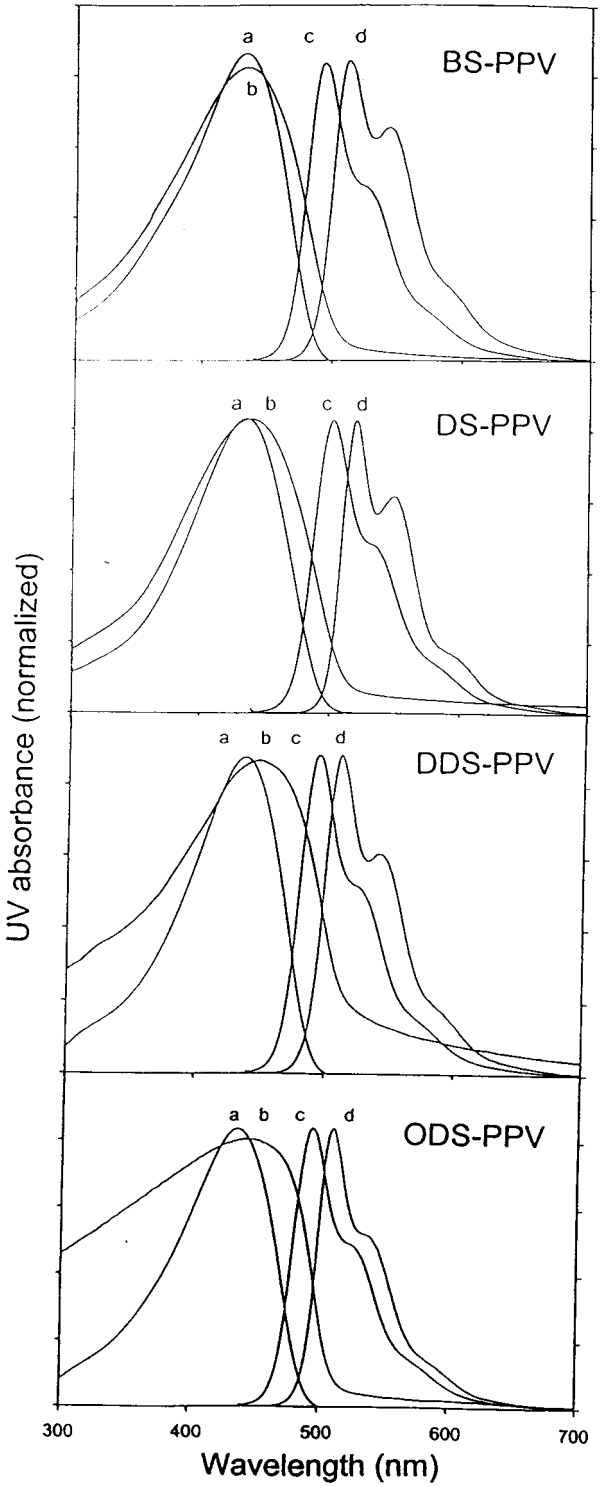

Figure 4. UV−vis absorption and photoluminescence spectra of Si-PPVs in solution and in solid state. (a) UV (solution); (b) UV (film); (c) PL (solution); (d) PL (film).

bathochromic shift of the film samples suggests that the long side chains benefit the polymer backbone in more planar conformation, which extends the conjugation length of the π electrons. The broader peak means that there are more energy levels corresponding to the $\pi-\pi^*$ transition for the long side chain bearing polymers. Band gaps of the polymers are estimated from the absorption edges to be 2.42−2.45 eV. Comparison of the UV−vis absorption spectra to that of poly[2-butyl-5-(2′-ethylhexyl)-1,4-phenylenevinylene] (BuEH-PPV),[33] which is a typical alkyl-substituted green-light-emitting PPV

Table 2. Optical Properties of Si-PPVs

polymer	λ_{max} (UV, nm) solution	λ_{max} (UV, nm) film	λ_{max} (PL, nm) solution[a]	λ_{max} (PL, nm) film	FWHM (PL, nm) solution	FWHM (PL, nm) film	E_g (eV, UV/nm)	PL efficiency (solution, %)
BS-PPV	434	434	494 (526)	512 (543)	59	64	2.45 (506)	87
DS-PPV	435	439	501 (535)	520 (548)	59	57	2.42 (512)	86
DDS-PPV	436	448	494 (523)	511 (540)	59	61	2.43 (510)	87
ODS-PPV	435	445	494 (527)	510 (536)	59	54	2.43 (510)	89

[a] Shoulder peak.

derivative with quite high PL efficiency (solution 75% and film 62%), showing the λ_{max} at 422 nm and a band gap of 2.38 eV, respectively, the polymers reported here demonstrate larger λ_{max} and a little larger band gap. The red shift of λ_{max} of the silyl-substituted PPVs compared to that of BuEH-PPV can be ascribed to two factors: the first is the contribution of the slightly electron-donating character of the silicon atom;[34] the second is concerned with the conjugation extension from the phenylene ring to the silicon through $\pi-d_{Si}$ or $\pi-\sigma$ interaction, which can lower the energy gap of the $\pi-\pi^*$ transition of the polymer main chain.[35] The conjugation extension through $\pi-d_{Si}$ or $\pi-\sigma$ interaction was observed in several π-conjugated polymers incorporating organosilicon bridging units in the skeleton.[14,15] The little larger band gaps of the Si-PPVs than BuEH-PPV result from the greater hindrance effect of the bulky substitution of silyl groups than the two alkyl groups, which leads to twisting of the polymer main chains. From the comparison of the maximum and the edge absorption of the Si-PPVs and BuEH-PPV, it can be seen that Si-PPVs show narrower absorption bands, which indicates that the polymers are more homogeneous than the dialkyl-substituted PPVs.

PL spectra of Si-PPVs in solution exhibit maximum peaks at 494 nm except DS-PPV, which shows the peak at a little lower energy region with λ_{max} at 501 nm. All the PL spectra reveal a shoulder around 530 nm and a weak tailed emission in the region of 560−600 nm. The wavelengths of the peaks are summarized in Table 2. The spectra of the film samples resembled their solution ones, shifted to a longer wavelength region, and demonstrated a clearer side peak. The maximum emission peaks and the side peaks are at about 510 and 540 nm, respectively, which correspond to the green emission. The fine structures of the emission spectra of both the solution and film samples are associated with the vibronic coupling of the excitons. The energy spaces between the main peaks and the shoulders are about 120−140 meV, which are in respect to the vibrational energy of carbon−carbon or carbon−silicon bond stretching.[36] It can be seen that all the emission spectra are very sharp. The solution ones demonstrate the full width at half-maximum (FWHM) of 59 nm, while the film samples lie in the range of 54−64 nm. In comparison with the FWHM of BuEH-PPV films (82 nm), the sharper emission indicates the emission color contains more greenish component and less yellow one, which is one of the desirable features for realizing three pure primary colors for display technology. Although the emission bands are all very sharp for the four polymers, and the overlap of the emission and absorption spectra is quite narrow, it is worth noting that the overlapping area of the film samples slightly grows with increasing side chain length due to the broadening of the absorption spectra of the long side chain polymers. From the viewpoint of self-absorption, the polymers used as the active materials of PLEDs should avoid the optical spectra overlapping. Therefore, polymers of BS-PPV or DS-PPV are better than other two polymers with longer side chains.

The PL quantum yields of the Si-PPVs in chloroform (ca. 1×10^{-6} M) were measured by comparing to quinine sulfate (ca. 1×10^{-5} M) in 0.10 M H_2SO_4 as standard. The quantum efficiencies of Si-PPVs after refractive index correction can be calculated according to eq 1,[37]

$$\phi_{unk} = \phi_{std}\left(\frac{I_{unk}}{I_{std}}\right)\left(\frac{A_{std}}{A_{unk}}\right)\left(\frac{\eta_{unk}}{\eta_{std}}\right)^2 \quad (1)$$

where ϕ_{unk}, ϕ_{std}, I_{unk}, I_{std}, A_{unk}, A_{std}, η_{unk}, and η_{std} are the fluorescent quantum yields, the integration of the emission intensities, the absorbances at the excitation wavelength, and the refractive indexes of the corresponding solutions for the samples and the standard, respectively. Here we use the refractive indexes of the pure solvents as those of the solutions.

Assuming the PL_{eff} of quinine sulfate in 0.10 M H_2SO_4 solution of 0.546 at 365 nm excitation,[37b] the refractive indexes of polymer dilute solutions in chloroform and 0.10 M H_2SO_4 are 1.446 and 1.333 respectively; the quantum yields of the Si-PPVs were determined to be as high as 86%−89%, which are higher than those of BuEH-PPV (PL_{eff} of solution 75%), poly[2,5-bis-(cholestanoxy)-1,4-phenylenevinylene] (BCHA-PPV, PL_{eff} of solution 78%),[33] or some recently reported diphenyl-substituted PPVs.[38] It seems that the side chain length does not affect the quantum yields of the solution samples. For film samples, we can expect that the polymers would have high quantum efficiencies although the polymers bear symmetric side chains. It is reported that the film PL_{eff} can be increased by separating the conjugated backbones in all three dimensions, while the better packing of the polymer chains will reduce its quantum efficiency.[39] In Si-PPVs, the bulky dimethylalkylsilyl groups linked to the phenylene rings will twist the backbone and prevent close packing of the conjugated chains, which act as BCHA-PPV or BuEH-PPV. Therefore, such bulky symmetric substitution will not lower the polymer quantum efficiencies in the film state.

When materials are used as the emissive layer for PLEDs, matches of their HOMO and LUMO energy levels with work functions of electrodes as well as their optical, electrical, and chemical stability are of paramount importance. The electronic energy levels of the polymer will directly determine the PLED device configuration, which is associated with device structure design and selection of electrode materials and charge-transporting materials, whereas the stability is related to the device lifetime in operation. Usually the ionization potential (IP, i.e., the highest occupied molecular orbitals (HOMO) of an organic molecule) is measured by ultraviolet photoelectron spectroscopy (UPS). The electron affinity (EA, i.e., the lowest unoccupied molecular orbitals (LUMO) of the organic molecule) is deduced

from the IP value and the band gap obtained from optical absorption spectra, which is not a direct measuring means. CV is a facile and effective approach to measure the redox reversibility, reproducibility, and stability of polymer films on electrodes, and it can be deployed to simultaneously evaluate both the HOMO and LUMO energy levels and the band gap of a polymer. The electrochemical processes are similar to the situation of charge injection and transport in LED devices. Therefore, it is a simple and useful technique to measure the HOMO and LUMO energy levels of a polymer. According to the empirical relationship proposed by Bredas et al,[40] the solid state IP and EA have a correlation to the E'_{ox} and E'_{red} of the onset potentials vs SCE of oxidation and reduction processes of a polymer. The onset potentials are determined from the intersection of the two tangents drawn at the rising current and baseline charging current of the CV traces. The correlation can be expressed as

$$\mathrm{IP} = -(E'_{ox} + 4.4)\ \mathrm{eV} \quad (2)$$

$$\mathrm{EA} = -(E'_{red} + 4.4)\ \mathrm{eV} \quad (3)$$

Figure 5 demonstrates the cyclic voltammograms of Si-PPVs in 0.10 M tetrabutylammonium tetrafluoroborate (Bu_4NBF_4) in acetonitrile, which were performed in a three-electrode cell. The polymer films were prepared by dip-coating the polymer chloroform solution (10 mg/mL) on a Pt electrode (0.50 × 0.50 cm^2 with area of 0.50 cm^2 for both sides) and dried in argon. The polymer films were scanned anodically and cathodically separately. During the cathodic scan, the polymers all exhibited reversible *n*-doping processes. $E_{c/a}$ were around −2.0/−1.8 V vs SCE. Along with the potential scan, the color of the films changed from green to purple or alike, then to brown or yellow after oxidation, which depends on the polymer structure. The onsets for the n-doping processes are about −1.8 V. Although the onset potentials are quite similar, it can be found that the peak potential is further negative with the side chain length increase. Meanwhile, the peak current is drastically decreased when the side chain changed from C4 to C10 or longer. This result indicates that the polymer with longer side chains needs more potential to be reduced. In other words, the polymer film with long side chains will be more difficult to accept or transport electrons than short side chain bearing polymers.

When an anodic scan was performed, the Si-PPVs showed irreversible p-doping processes. The peak potentials are about 1.4 V, accompanied by the color changes with the charging and discharging processes. The observation of irreversible p-doping may be attributed to instability of the doped state. The onset potentials of the polymers are in the range of 1.12−1.22 V. It can be seen that the peak potential and the onset potential for ODS-PPV is a little higher than the others. From the CV curves of the p-doping, it can be found that the peak current demonstrates an obvious trend—the peak current is dramatically decreased with the side chain length increase. This result also implies that increasing the side chain length of the polymers will increase the energy barrier for the anodic reaction. The decreasing peak current for longer side chain bearing polymers is reasonable: during oxidation the counterions will diffuse from the bulk electrolyte solution to the oxidation site to balance the charges. The longer the side chain the polymer bears, the more difficult for the counterions to migrate. Another reason is the charge transport from the polymer to the electrode (or vice versa) will be arduous for longer side chain polymers. The reproducibility investigation indicates that all the processes, either p-doping or n-doping, can be run up to five cycles without obvious change in the shape of the CV traces. However, the anodic currents of BS-PPV and DS-PPV as well as both the cathodic and anodic currents for DDS-PPV and ODS-PPV decreased by degrees with the repeated cycles. The results suggest that the electrochemical stability of the Si-PPVs is better for the shorter side chain polymers than for the longer ones. The efficiency of PLEDs depends on a combination of PL efficiency, balance of charge injection and transporting, and carrier mobility of an active material. A longer long side chain of the polymer may affect

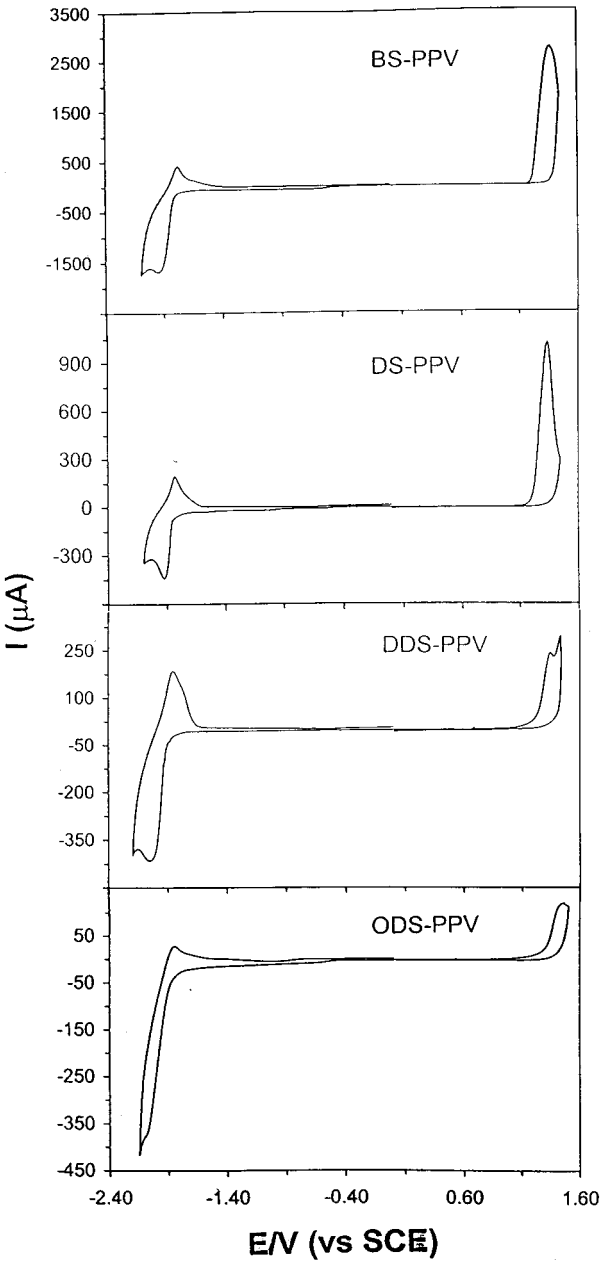

Figure 5. Cyclic voltammograms of Si-PPVs films dip-coated on platinum plate electrodes in acetonitrile containing 0.10 M Bu_4NBF_4. Platinum wire as the counter electrode. The potentials reference against Ag/0.10 M $AgNO_3$ in acetonitrile. Scan rate 10 mV/s.

Table 3. Electrochemical Properties and Energy Levels of Si-PPVs

polymer	$E_{c/a}$ (V)	$E_{a/c}$ (V)	color change (p-doping)	color change (n-doping)	E_{Ox} (onset, V)	E_{Red} (onset, V)	E_g (eV, Echem)	IP (eV)	EA (eV)
BS-PPV	−1.95/−1.78	1.37	green/blue green/yellow green	green/purple/brown	1.14	−1.80	2.94	−5.54	−2.60
DS-PPV	−1.92/−1.83	1.33	green/blue/yellow green	green/purple blue/brown	1.12	−1.78	2.90	−5.52	−2.62
DDS-PPV	−2.06/−1.85	1.33	green/green blue/yellow green	green/blue purple/yellow	1.16	−1.82	2.98	−5.56	−2.58
ODS-PPV	−2.09/−1.84	1.46	green/blue green/yellow green	green/dark blue/brown	1.22	−1.78	3.00	−5.62	−2.62

the charge mobility in the device, which was demonstrated in a comparison study among MEH-PPV, BuEH-PPV, and BCHA-PPV.[33] In this series of polymers, BCHA-PPV, with the most bulky substituent, shows the lowest EL efficiency in double-layer devices with configuration of ITO/PVK/polymer/Ca although its film PL efficiency is higher than MEH-PPV and close to BuEH-PPV. Therefore, we may infer that BS-PPV and DS-PPV will have a better performance than DDS-PPV or ODS-PPV in PLED applications.

From the onset potentials of the oxidation and reduction processes, it can be estimated that the band gaps of Si-PPVs are from 2.90 to 3.00 eV, which are higher than the values obtained from the optical absorption spectra. The difference may be caused by the interface barrier between the polymer film and the electrode surface. The electrochemical datum may be the combination of the optical band gap and the interface barrier for charge injection, which makes it larger. However, the band gap obtained from the electrochemical method should be more meaningful as a reference for PLED device design due to similar configuration between the electrochemical system and practical PLED devices. According to the relationship described above and the onset potentials listed in Table 3, the IP and EA values for the four polymers were estimated. All the data, including IP and EA values, electrochemical band gaps, oxidation and reduction onset potentials, n-doping and p-doping peak potentials, and the color changes during the processes, are listed in Table 3. Comparing the EA and IP values of Si-PPVs to PPV, which are −2.5 and −5.0 eV, respectively,[41] it can be seen that the Si-PPVs have negatively higher values of EA, which means that for the polymers the electron injection process is easier than that of PPV. However, the IP values are much more negative than that of PPV, suggesting that holes are difficult to be injected from ITO into the polymers when they are used as the active layer for single-layer devices. Due to the retarded injection of holes from ITO, the imbalance situation of the energy barriers for hole and electron injection into alkyl- or alkoxy-substituted PPVs may be improved by the replacement of Si-PPVs as the active layer for single-layer devices, using air-stable metal as the cathode. These data of energy levels are consistent with the performance of monosilylated PPV (poly(2-dimethyloctylsilyl-1,4-phenylenevinylene), DMOS-PPV) based single-layer devices reported by Friend et al.[19] The single-layer device of ITO/DMOS-PPV/Al yielded a remarkably high external quantum efficiency of 0.05%. However, when Al was replaced by Ca, an efficient electron injection electrode, the efficiency was only increased a bit to 0.08% with an increased current density. The device performance implies that the holes and electrons in the Al device are more balanced. In addition, there may be another possibility that the efficiency of Si-PPV based devices is determined by hole injection instead of electron injection. The results of electrochemical investigations described above reinforce this point. To verify the hypothesis, single-layer devices and double-layer devices each with a hole injection layer were fabricated and evaluated using DS-PPV as the emissive layer.

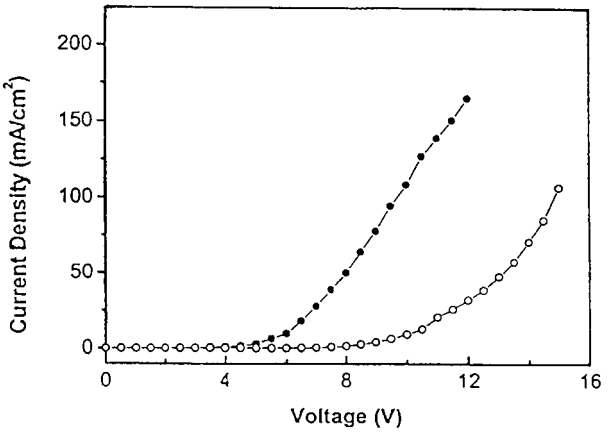

Figure 6. Current−voltage characteristics for ITO/DS-PPV/Mg:Ag (open cycle) and ITO/PEDOT:PSS/DS-PPV/Mg:Ag (filled cycle).

Since the effect of cathode materials from Al to Ca on the efficiency of DMOS-PPV is not obvious,[19] Mg:Ag alloy (10:1 by mass) with the work function lying between Ca and Al was used as the cathode. The configuration of the single-layer and double-layer devices is ITO/DS-PPV/Mg:Ag and ITO/PEDOT:PSS/DS-PPV/Mg:Ag, respectively. The thickness of the emissive layer is 60 nm for both devices, while the thickness of the hole injection layer of PEDOT:PSS is 30 nm. The curent−voltage characteristics measured for the devices are depicted in Figure 6. A forward bias current was obtained when the ITO electrode was the positive electrode and Mg:Ag was grounded. The current density increased with an increase in the forward bias, and the curve demonstrated a typical diode character. Under a forward bias, the emitting light from the single-layer device and the double-layer device becomes visible at 7.5 and 4.0 V, respectively. Comparison of the turn-on voltage of the single-layer device with the reported work cited in ref 19, the result is much better than the latter one, which showed a threshold voltage of 15 V with a similar thickness of the emissive layer. We can also see that introduction of a hole injection layer can largely lower the turn-on voltage of the resulting device. Preliminary efficiency measurement of the two types of devices indicates that the maximum current efficiency and power efficiency are 0.3 cd/A and 0.09 lm/W for the single-layer device and 2.3 cd/A and 0.65 lm/W for the double-layer device. The addition of the hole injection layer leads to the efficiency improved about 7-fold. The results proved the deduction from electrochemical analysis that introduction of silyl groups into PPVs will retard the hole injection ability and the anode modification will be the key factor for device performance. A detailed device evaluation will be reported elsewhere.

Conclusions

A series of silyl-substituted poly(*p*-phenylenevinylene)s (Si-PPVs), with the side chain length ranged

from C1 to C18, was synthesized through the Gilch route. The polymers, except MS-PPV, show good solubility, good film-forming ability, and amorphous properties due to the branching structure of dimethylalkylsilyl groups linked to the polymer backbone as well as enhanced flexibility of side chain originated from the larger size of Si atom and longer bond length of C−Si compared with corresponding carbon or oxygen counterparts. The polymers demonstrate high thermal stability with the onset degradation temperature around 300 °C. Weight loss percentage analysis and FT-IR spectroscopic analysis of the thermolysis residues indicated that the polymers with long side chains will lose one side group and the long aliphatic chain linked to the other Si atom in the first stage accompanied by partially oxidation of the carbon in the atmosphere of air.

UV−vis spectra of the solution samples for the four soluble polymers are quite similar, whereas the film samples demonstrate the broadening effect with increase of the side chain length. The electronic effect of the silyl group substitution on PPV originates from two factors. One is the weak electron-donation effect of Si atom and the conjugation extension from the polymer backbone to the silicon atom through $\pi-d_{Si}$ or $\pi-\sigma$ interaction, which makes the absorption peak red shifted compared with alkyl-substituted PPVs such as BuEH-PPV. The other is the steric hindrance effect of the branching of the side chains close to the polymer backbone, which leads to increases of the polymer band gaps compared with the respective reference polymer. The PL spectra are also quite similar for both the solution and film samples. The emission spectra of the film samples are much narrower and lie in the region of green. The PL efficiencies of all the solution samples are close to 90%. However, the performance of shorter side chain bearing polymers may be better when they are used to fabricate LED devices due to the lower proportion of the side chains occupied in the whole polymer.

The HOMO and LUMO energy levels of the polymers were evaluated through CV. CV measurements also indicate that all the polymers exhibit reversible n-doping processes and irreversible p-doping processes. With the side chain length increase, the polymer film can be reduced or oxidized at higher potentials. Meanwhile, the peak current will dramatically decrease, which means the charge injection and/or transporting is retarded due to the longer side chains. This property may result in a low EL quantum efficiency when the longer side chain bearing polymers are used as the active layer of LED devices due to the lower charge mobility and the lower proportion of the main chain occupied in the polymer. In terms of stability and reproducibility, polymers with shorter side chains are better than longer ones. From the energy levels derived from the onset potentials, it can be seen that the electron affinity of the silyl-substituted PPVs is similar to that of PPV or alkyl/alkoxy-substituted PPVs, while the ionization potentials are much more negative than the reference polymers. The IP and EA values of the Si-PPVs suggest that better performance of LED devices be expected using Si-PPVs as the active layer to fabricate single-layer devices with air-stable metal cathode, or the device performance may be improved by modifying the anode. The device fabrication and evaluation using DS-PPV as the emissive layer and Mg:Ag as the cathode demonstrated that hole injection is a key factor for the device performance, and addition of a thin layer of PEDOT:PSS can improve the current efficiency and power efficiency by about 7-fold and largely lower the turn-on voltage of the devices.

Supporting Information Available: Synthesis, purification, and characterization of **2a**, **2b**, **2d**, **2e**, **3a**, **3b**, **3d**, **3e**, **4a**, **4b**, **4d**, and **4e** (5 pages). This material is available free of charge via the Internet at http://pubs.acs.org.

References and Notes

(1) (a) Friend, R. H.; Gymer, R. W.; Holmes, A. B.; Burroughes, J. H.; Marks, R. N.; Taliani, C.; Bradley, D. D. C.; Dos Santos, D. A.; Bredas, J. L.; Logdlund, M.; Salaneck, W. R. *Nature* **1999**, *397*, 121. (b) Cao, Y.; Parker, I. D.; Yu, G.; Zhang, C.; Heeger, A. J. *Nature* **1999**, *397*, 414.

(2) Halls, J. J. M.; Walsh, C. A.; Greenham, N. C.; Marseglia, E. A.; Friend, R. H.; Moratti, S. C.; Holmes, A. B. *Nature* **1995**, *376*, 498.

(3) Garnier, F.; Hajlaoui, R.; Yassar, A.; Srivastava, P. *Science* **1994**, *265*, 1684.

(4) Burroughes, J. H.; Bradley, D. D. C.; Brown, A. R.; Marks, R. N.; Mackay, K.; Friend, R. H.; Burn, P. L.; Holmes, A. B. *Nature* **1990**, *347*, 539.

(5) Kraft, A.; Grimsdale, A. C.; Holmes, A. B. *Angew. Chem., Int. Ed.* **1998**, *37*, 402.

(6) Segura, J. L. *Acta Polym.* **1998**, *49*, 319.

(7) (a) Gustafsson, G.; Cao, Y.; Treacy, G. M.; Klavetter, F.; Colaneri, N.; Heeger, A. J. *Nature* **1992**, *357*, 477. (b) Greenham, N. C.; Moratti, S. C.; Bradley, D. D. C.; Friend, R. H.; Burn, P. L.; Holmes, A. B. *Nature* **1993**, *365*, 628.

(8) (a) Grem, G.; Leditzky, G.; Ullrich, B.; Leising, G. *Adv. Mater.* **1992**, *4*, 36. (b) Yang, Y.; Pei, Q.; Heeger, A. J. *J. Appl. Phys.* **1996**, *79*, 934.

(9) Berggren, M.; Inganas, O.; Gustafsson, G.; Rasmusson, J.; Andersson, M. R.; Hjertberg, T.; Wennerstrom, O. *Nature* **1994**, *372*, 444.

(10) (a) Ohmori, Y.; Uchida, M.; Muro, K.; Yoshino, K. *Jpn. J. Appl. Phys.* **1991**, *30*, L1941. (b) Pei, Q.; Yang, Y. *J. Am. Chem. Soc.* **1996**, *118*, 7416.

(11) Yu, W.-L.; Meng, H.; Pei, J.; Huang, W. *J. Am. Chem. Soc.* **1998**, *120*, 11808.

(12) Kim, K. D.; Park, J. S.; Kim, H. K.; Lee, T. B.; No, K. T. *Macromolecules* **1998**, *31*, 7267.

(13) (a) Li, H.; West, R. *Macromolecules* **1998**, *31*, 2866. (b) Miller, R. D.; Michl, J. *Chem. Rev.* **1989**, *90*, 1359.

(14) Ohshita, J.; Kunai, A. *Acta Polym.* **1998**, *49*, 379.

(15) (a) Herrema, J. K.; Hutten, P. F.; Gill, R. E.; Wildeman, J.; Wieringa, R. H.; Hadziioannou, G. *Macromolecules* **1995**, *28*, 8102. (b) Garten, F.; Hilberer, A.; Cacialli, F.; Esselink, E.; Dam, Y.; Schlatmann, B.; Friend, R. H.; Klapwijk, T. M.; Hadziioannou, G. *Adv. Mater.* **1997**, *9*, 127. (c) Tang, H. Q.; Zhu, L. H.; Harima, Y.; Yamashita, K.; Ohshita, J.; Kunai, A. *J. Polym. Sci. Part B, Polym. Phys.* **1999**, *37*, 1873.

(16) Kim, H. K.; Ryu, M. K.; Kim, K. D.; Lee, S. M.; Cho, S. W.; Park, J. W. *Macromolecules* **1998**, *31*, 1114.

(17) Hoger, S.; McNamara, J. J.; Schricker, S.; Wudl, F. *Chem. Mater.* **1994**, *6*, 171.

(18) Zhang, C.; Hoger, S.; Pakbaz, K.; Wudl, F.; Heeger, A. J. *J. Electron. Mater.* **1994**, *23*, 453.

(19) Kim, S. T.; Hwang, D. H.; Li, X. C.; Gruner, J.; Friend, R. H.; Holmes, A. B.; Shim, H. K. *Adv. Mater.* **1996**, *8*, 979.

(20) Hwang, H.; Kim, S. T.; Shim, H. K.; Holmes, A. B.; Moratti, S. C.; Friend, R. H. *Chem. Commun.* **1996**, 2241.

(21) Chuah, B. S.; Hwang, D. H.; Kim, S. T.; Moratti, S. C.; Holmes, A. B.; DeMello, J. C.; Friend, R. H. *Synth. Met.* **1997**, *91*, 279.

(22) Corey, J. Y. History Overview and Comparison of Silicon with Carbon. In *The Chemistry of Organic Silicon Compounds, Part I*; Patai, S., Rappoport, Z., Eds.; John Wiley and Sons Ltd.: New York, 1989; Chapter 1, pp 1−56.

(23) Gerns, F. R. U.S. Patent 3932542, 1976.

(24) Kang, I. N.; Hwang, D. H.; Shim, H. K.; Zyung, T.; Kim, J. J. *Macromolecules* **1996**, *29*, 165.

(25) (a) Wudl, F.; Srdanov, G. U.S. Patent 5189136, 1990. (b) Wudl, F.; Hoger, S. U.S. Patent 5679757, 1993.

(26) (a) Gruter, G. J. M.; Akkerman, O. S.; Bickelhaupt, F. *J. Org. Chem.* **1994**, *59*, 4473. (b) Walling, C.; Rieger, A. L.; Tanner, D. D. *J. Am. Chem. Soc.* **1963**, *85*, 3129.

(27) (a) Gelinck, G. H.; Warman, J. M.; Staring, E. G. J. *J. Phys. Chem.* **1996**, *100*, 5485. (b) Spreitzer, H.; Becker, H.; Kluge, E.; Kreuder, W.; Schenk, H.; Demandt, R.; Schoo, H. *Adv. Mater.* **1998**, *10*, 1340.
(28) Smith, A. L. *J. Chem. Phys.* **1953**, *18*, 1997.
(29) Williams, E. A. NMR Spectroscopy of Organosilicon Compounds. In *The Chemistry of Organic Silicon Compounds,Part I*; Patai, S., Rappoport, Z., Eds.; John Wiley & Sons Ltd.: New York, 1989; Chapter 8, p 511.
(30) Becker, H.; Spreitzer, H.; Ibrom, K.; Kreuder, W. *Macromolecules* **1999**, *32*, 4925.
(31) Becker, H.; Spreitzer, H.; Kreuder, W.; Kluge, E.; Schenk, H.; Parker, I.; Cao, Y. *Adv. Mater.* **2000**, *12*, 42.
(32) Silverstein, R. M.; Bassler, G. C.; Morrill, T. C. *Spectrometric Identification of Organic Compounds*, 5th ed.; John Wiley & Sons Inc.: New York, 1991; Chapter 5.
(33) Andersson, M. R.; Yu, G.; Heeger, A. J. *Synth. Met.* **1997**, *85*, 1275.
(34) Vanhutten, P. F.; Gill, R. E.; Herrema, J. K.; Hadziioannou, G. *J. Phys. Chem.* **1995**, *99*, 3218.
(35) (a) Sakurai, H.; Sugiyama, H.; Kira, M. *J. Phys. Chem.* **1990**, *94*, 1837. (b) Shizuka, H.; Sato, Y.; Ueki, Y.; Ishikawa, M.; Kumada, M. *J. Chem. Soc., Faraday Trans. 1* **1984**, *80*, 341.
(36) (a) Bredas, J. L.; Cornil, J.; Heeger. A. J. *Adv. Mater.* **1996**, *8*, 447. (b) Hernandez, V.; Castiglioni, C.; Del Zoppo, M.; Zerbi, G. *Phys. Rev. B* **1994**, *50*, 9815.
(37) (a) Joshi, H. S.; Jamshidi, R.; Tor, Y. *Angew. Chem., Int. Ed.* **1999**, *38*, 2722. (b) Demas, J. N.; Crosby, G. A. *J. Phys. Chem.* **1971**, *75*, 991.
(38) Peng, Z. H.; Zhang, J. H.; Xu, B. B. *Macromolecules* **1999**, *32*, 5162.
(39) Andersson, M. R.; Berggren, M.; Olinga, T.; Hjertberg, T.; Inganas, O.; Wennerstrom, O. *Synth. Met.* **1997**, *85*, 1383.
(40) (a) Bredas, J. L.; Silbey, R.; Boudreux, D. S.; Chance, R. R. *J. Am. Chem. Soc.* **1983**, *105*, 6555. (b) deLeeuw, D. M.; Simenon, M. M. J.; Brown, A. B.; Einerhand, R. E. F. *Synth. Met.* **1997**, *87*, 53.
(41) Colvin, V. L.; Schlamp, M. C.; Alivisatos, A. P. *Nature* **1994**, *370*, 354.

MA0005670